

UCC Library and UCC researchers have made this item openly available. Please [let us know](#) how this has helped you. Thanks!

Title	Drag force as a function of cross section and angle of attack. A hydraulic laboratory dataset for numerical validation
Author(s)	Desmond, Cian J.; Thiebaut, Florent; Murphy, Jimmy
Publication date	2019-10-03
Original citation	Desmond, C. J., Thiebaut, F. and Murphy, J. (2019) 'Drag force as a function of cross section and angle of attack. A hydraulic laboratory dataset for numerical validation', Data in Brief, 27, 104596. (9pp.) doi: 10.1016/j.dib.2019.104596
Type of publication	Article (peer-reviewed)
Link to publisher's version	http://dx.doi.org/10.1016/j.dib.2019.104596 Access to the full text of the published version may require a subscription.
Rights	©2019 Published by Elsevier Inc. This is an open access article under the CC BY-NC-ND license (http://creativecommons.org/licenses/by-nc-nd/4.0/).Data in brief 27 (2019) 104596 http://creativecommons.org/licenses/by-nc-nd/4.0/
Item downloaded from	http://hdl.handle.net/10468/9316

Downloaded on 2020-06-06T01:24:01Z



UCC

University College Cork, Ireland
Coláiste na hOllscoile Corcaigh



ELSEVIER

Contents lists available at ScienceDirect

Data in brief

journal homepage: www.elsevier.com/locate/dib



Data Article

Drag force as a function of cross section and angle of attack. A hydraulic laboratory dataset for numerical validation



Cian J. Desmond^{*}, Florent Thiebaut, Jimmy Murphy

University College Cork, Marine and Renewable Energy, Ireland

ARTICLE INFO

Article history:

Received 9 April 2019

Received in revised form 9 September 2019

Accepted 24 September 2019

Available online 3 October 2019

Keywords:

Hydraulics

Fluid mechanics

CFD

Validation

Drag

Reynold's number

ABSTRACT

This data relates to a set of hydraulic laboratory experiments in which the flow around four cross-sections was investigated. Each cross section was examined at four angles of attack (0, 5, 10, 90°), seven velocities (0–0.7 m/s in 0.1 m/s steps) and two flow directions. The data is primarily from an array of load cell which monitored the loading on the cross-sections during testing in six degrees of freedom during testing. Video and photographs are also included.

© 2019 Published by Elsevier Inc. This is an open access article under the CC BY-NC-ND license (<http://creativecommons.org/licenses/by-nc-nd/4.0/>).

1. Data

A total of 4 folders:

01.Profiles -> CAD drawings of the 4 x profiles considered.

02.Data -> The raw experimental data.

03.Video -> Videos showing the experimental configuration.

04.Pictures -> General pictures taken during testing.

^{*} Corresponding author.

E-mail address: cian.desmond@ucc.ie (C.J. Desmond).

Specifications Table

Subject area	Civil Engineering
More specific subject area	Fluid mechanics, hydraulics.
Type of data	Load cell data.
How data was acquired	Load cells connected to a CompactRIO
Data format	Raw
Experimental factors	There is no pretreatment/filtering of these data.
Experimental features	An aluminum cross-section approximately 1 m in length was held between 2 flat plates connected to a moveable carriage in a wave basin. Under still water conditions, the cross section was moved through the wave basin. Data were collected from an array of load cells in 6 DoF. This process was repeated for four cross sections, each at 4 angles of attack and 7 velocities.
Data source location	University College Cork, Marine and Renewable Energy Ireland, Cork, Ireland.
Data accessibility	These data are publicly available for download: https://data.mendeley.com/datasets/2yzvjz6nvk/1

Value of the Data

These data could be used by any researcher working in the field of fluid mechanics or hydraulics to:

- **Why are these data useful?** -> These data are useful as they provide a comprehensive validation dataset to both numerical modelers and experimentalist working in the field of hydraulics.
- **Who can benefit from these data?** -> Researcher can use these data to validate their numerical models or to design their own experimental configurations. These data could also be used in the classroom to provide students with familiarity of working with experimental data and of the impact of cross-sectional area, angle of attack and velocity on drag.
- **How can these data be used for further insights and development of experiments?** -> The experimental configuration used, towing the cross-section in the tank, may not be optimal as it introduced vibrations into the system. An alternative would be to hold the cross section steady in a tank with current capabilities. This will however introduce additional turbulence to the system so a trade off exists. These data can be used to investigate this point.

In folder *02.Data*, there are sub-folders for each of the profiles described in *01.Profiles*. For each profile, data are provided as .txt for each angle of attack and velocity from 0.1 m/s to 0.7 m/s.

Within these .txt files, there is a timestamp followed by load data in N from 6 load cells. The position of these load cells on the frame supporting cross section are shown in the Fig. 1. The towing carriage mode in the positive x-direction during testing.

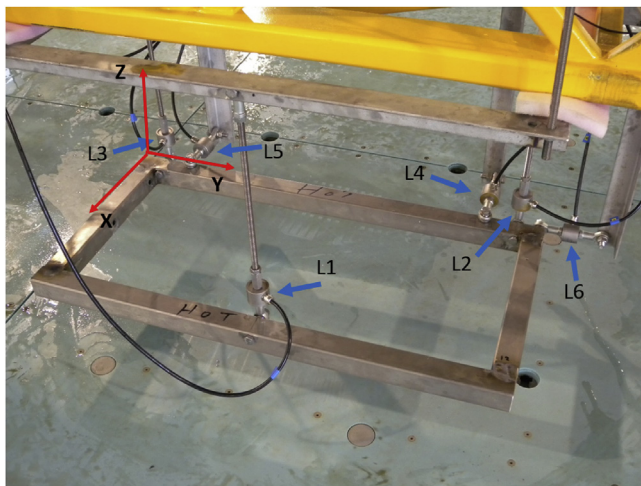


Fig. 1. Load cell positions.

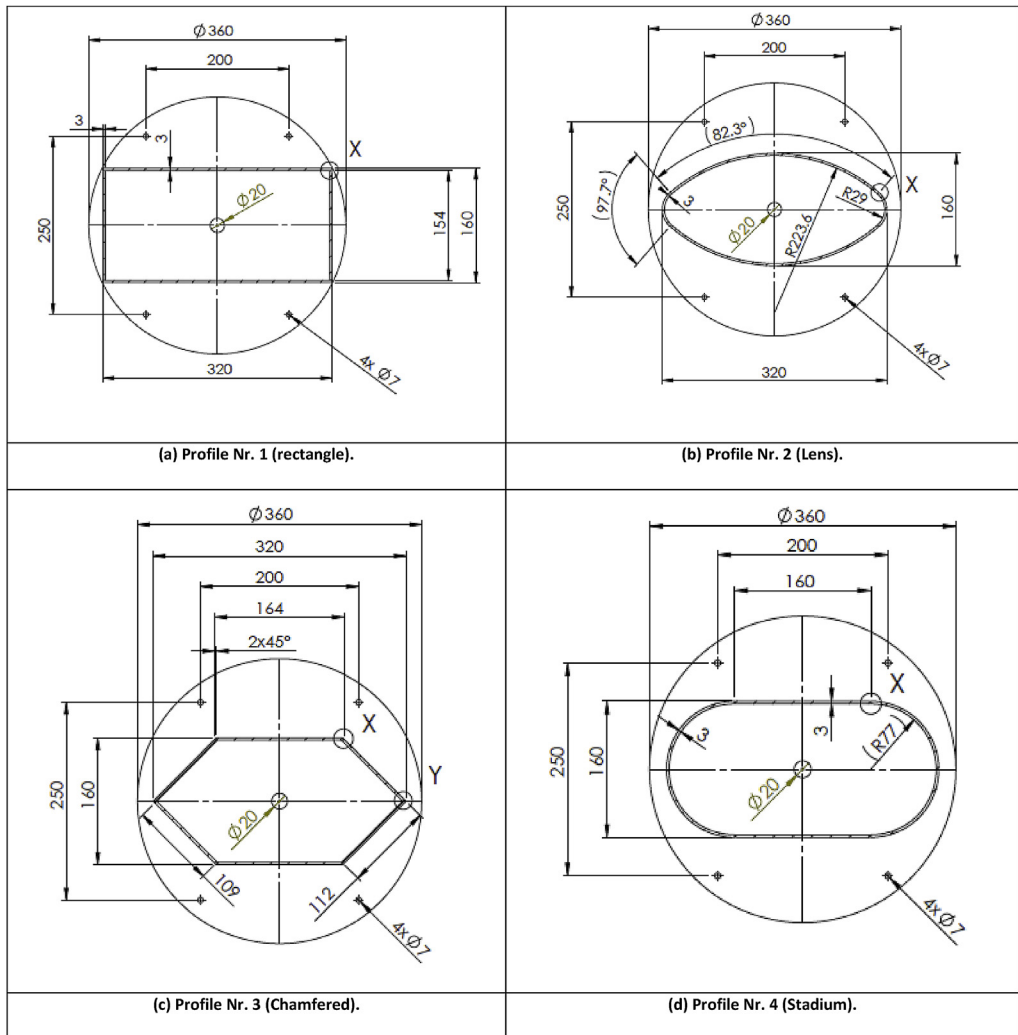


Fig. 2. Profiles dimension.

These data provide the instantaneous load in each degree of freedom for the profiles. An example dataset and guidance on interpretation is provided in Section 3.

2. Experimental design, materials, and methods

2.1. Profiles

A description of the four profiles tested, fabricated with aluminum, is shown in Fig. 2. Each profile is one meter in length and open with a 20 mm diameter hole on both sides to allow the profile to flood during testing.

During testing, the profiles were fixed on the holding frame (presented in the following section) so that the center of the profile was 530 mm below the water surface. These profiles were examined as a

fundamental research exercise in support of the development of the floating wind energy platform discussed in [1].

2.2. Towing bridge and holding frame

The towing bridge and holding frame are shown in Fig. 3 where only the parts above water level are visible. The two vertical plates are 1 m high and extend to a water depth of 710 mm. This allows the center of each profile to be placed at a depth of 530 mm. The sections underwater are shown in Fig. 4. The bridge spans across the basin, 850mm above the still water level. The holding frame is attached to the bridge above the center of the basin. It is composed of:

- An upper rigid frame fixed on the lower surface of the bridge.
- A lower rigid frame above the water with two vertical plates partly submerged where the profiles are attached.
- The two frames are connected via a series of six load transducers placed so that they allow the measurement of the 6° force transmission (linear loading and torque) between the two frames.



Fig. 3. View of the towing bridge and profile holding structure.

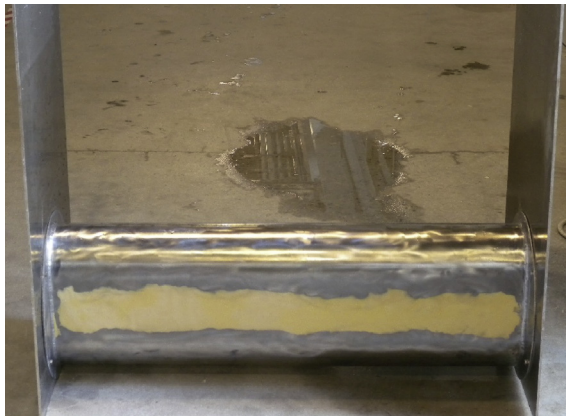


Fig. 4. Profile outside the water with vertical holding plates before being attached to the towing bridge.

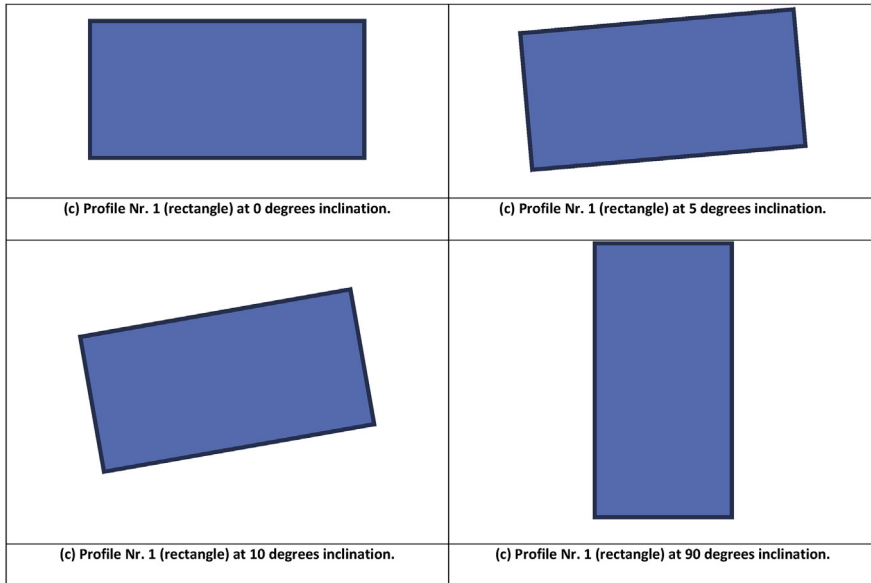


Fig. 5. Illustration of the four inclinations tested.

The vertical holding plates were perforated for ease of installation of the profiles at the 4 required angles, 0, 5, 10 and 90° as illustrated in Fig. 5.

3. Setup and methodology

3.1. Deep ocean basin specification

The profiles were tested in the Deep Ocean Basin of the Lir NOTF. The basin, shown in Figs. 6 and 7, has dimensions of 35 m long x 12 m wide x 3 m deep. The basin is equipped with 16 hinged force



Fig. 6. Lir NOTF deep ocean basin.

feedback paddles capable of a peak wave generation condition of $H_s = 0.6$ m, $T_p = 2.7$ s and $H_{max} = 1.1$ m. A movable floor plate allows the water depth to be adjusted to a maximum of 3 m. During these tests, the tank water depth was set to 3 m in order to minimize its influence on the water flow around the model.

3.2. Load measurement structure

The load measurement system is composed of 6 load transducers placed on the holding frame between the towing bridge and the model. It allows the measurement of the 6° load applied on the frame due to its weight, inertia and hydrodynamic forces. However, in order to calculate the drag and lift forces, the effect of the weight on each vertical load cell is deducted for each test as an offset. Each test is carried out at a constant speed and hence inertia forces are minimal.

The 6 load cells on the holding frame are shown in Fig. 8 and their attachment points location on the lower part of the frame is given in Table 1. In this table, the origin is at the top of the frame corner near the “L3” load cell as shown in red in Fig. 8. The X axis is pointing towards the basin paddles (drag motion direction), the Y axis is pointing towards the West wall and Z axis is vertical upwards.

The drag force can be calculated from the sum of load cells 4 and 5 and the lift force from the sum of load cell 1, 2 and 3.

3.3. Load cells

The six load cells used are 500 N Applied Measurement DDEN series. Section 3.2 describes the holding frame and load cells locations.

Prior to testing, each load cell was individually calibrated by hanging a series of known weights and recording the output in volts per volt excitation from the load cell. The results are then displayed on a graph for verification, Fig. 9 shows the calibration curve for the load cell number 1. The error in Newton was also calculated and the results are shown in Table 2 for the 6 load cells, L1 to L6. The maximum observed error is ± 0.3 N.

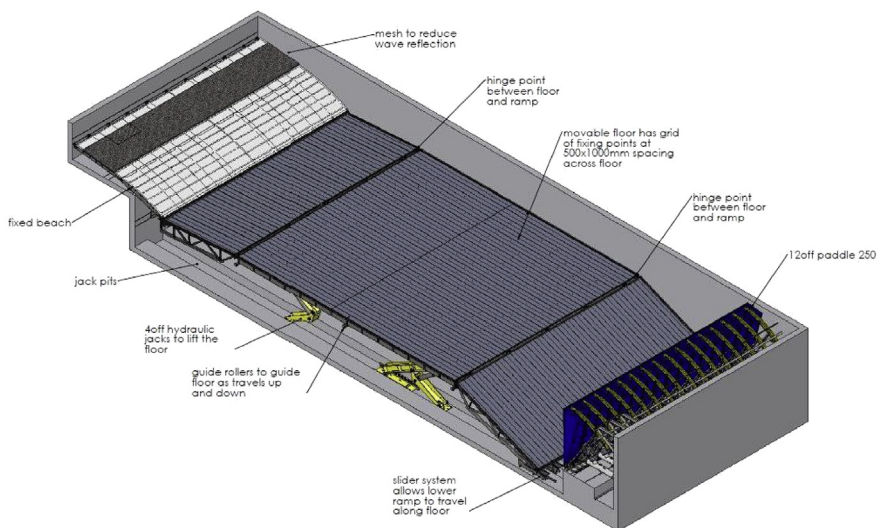


Fig. 7. Schematic view of the Lir NOTF Deep Ocean Basin.

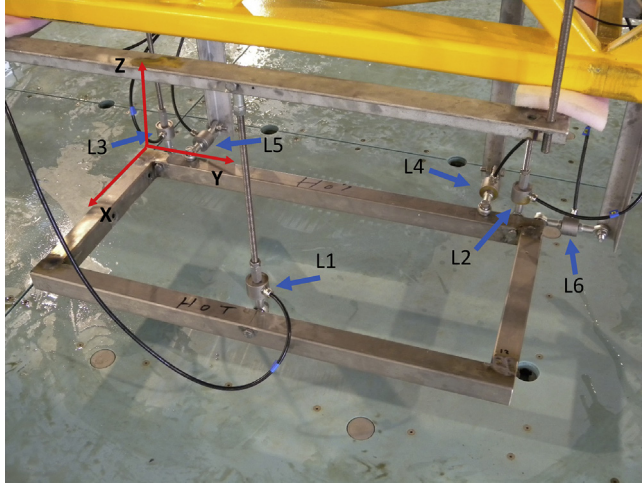


Fig. 8. Profile holding structure and load cells placements.

Table 1

List of load cells attachment locations on the lower frame.

Number	Orientation	Position on frame		
		X	Y	Z
1	Z	450	500	-12
2	Z	-8	935	-12
3	Z	-8	65	-12
4	X	12	865	8
5	X	12	135	8
6	Y	-8	988	-15
Profile Centre	-	500	250	-820
Water level	-	-	-	-290

3.4. Test methodology

During each tests, the profiles were driven under the towing bridge at a set speed from one side of the deep ocean basin to the other. The test is repeated for each profile and each angle of inclination for a range of speeds from 0.1 to 0.7 m/s. Each test includes two directions:

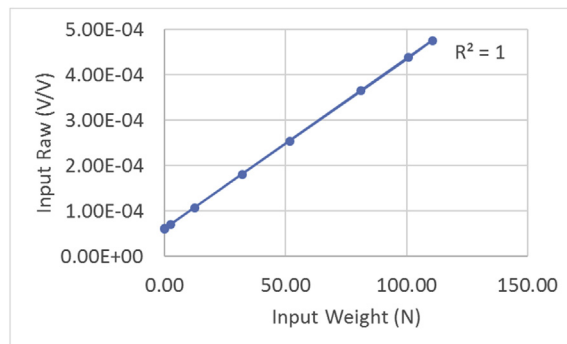
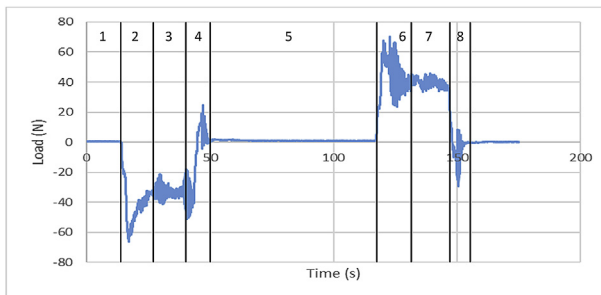


Fig. 9. Load cell number 1 calibration curve.

Table 2

Load cell calibration errors measured.

Load(N)	L1 (N)	L2 (N)	L3 (N)	L4 (N)	L5 (N)	L6 (N)
0.00	0.00	0.00	0.00	0.00	0.00	0.00
2.76	0.23	-0.02	0.01	0.00	-0.05	0.02
12.57	0.29	0.01	0.05	0.01	-0.01	0.01
32.19	0.30	0.07	-0.02	0.00	-0.02	-0.11
51.81	0.27	-0.02	0.09	-0.04	-0.06	-0.24
81.24	0.17	0.04	0.04	0.03	-0.01	-0.23
100.86	0.16	-0.04	0.09	0.01	-0.04	-0.18
110.67	0.00	0.00	0.00	0.00	0.00	0.00
0.00	0.16	-0.02	-0.05	-0.09	-0.07	-0.05

**Fig. 10.** Drag test, measurement description.

- Direction 1, from the beach side towards the paddles side
- Direction 2, from the paddle side towards the beach side

When the profiles are tested at 0 or 90° inclinations, the profiles are placed similarly in relation to the towing motion and hence this represents a repeat test.

When the profiles are placed at 5 or 10° the profile side facing the paddles is lower than the side facing the beach. Therefore, in direction 1 (towards the basin paddles) the angle of attack is negative and in direction 2 the angle of attack is positive.

Each test recorded can be described in 8 periods as described below and illustrated in Fig. 10:

1. an initial period at 0 speed
2. a transition period during acceleration
3. a steady state period of at least 15 seconds with constant speed towards the basin paddles
4. a transition period during deceleration
5. a settling period to allow water perturbations in the basin to dissipate
6. a transition period during acceleration
7. a steady state period of at least 15 seconds with constant speed towards the basin beach
8. a transition period during deceleration

Relatively high levels of noise were observed on the raw data collected when the bridge is in motion. This is mostly due the effect of the bridge vibration and can be significantly filtered using the average value of the steady state periods (number 3 and 7 in Fig. 10).

Acknowledgments

This experimental work was made possible with funding from the Sustainable Energy Authority of Ireland (SEAI). Sincere thanks to our industrial collaborators Bluwind Power Ltd. and aerodyn engineering gmbh for allowing these data to be made available to the research community.

Conflict of Interest

The authors declare that they have no known competing financial interests or personal relationships that could have appeared to influence the work reported in this paper.

Reference

- [1] C.J. Desmond, J.-C. Hinrichs, J. Murphy, Uncertainty in the physical testing of floating wind energy platforms: accuracy versus precision, *Energies* 12 (3) (2019) 14, <https://doi.org/10.3390/en12030435>. MDPI AG.